A High-gain, Low-profile Filtering Antenna Based on a Novel Metasurface

Jingci Zhu, Guanmao Zhang*, Zhihang Li, Zonge Che, Juan Yue, Yinhai Feng, Qian Zhang, and Rui Qiu

Institute of Optoelectronics and Electromagnetics Information,
School of Information Science and Engineering, Lanzhou University, Lanzhou 730000, China
*zhanggm@lzu.edu.cn

Abstract **–** In this paper, a filtering antenna based on a metasurface is designed using slot-coupled feeding, and the metasurface unit is a fractal pattern. Replacing the rectangular patch on the metasurface with a fractal patch can introduce a radiation zero point on the upper sideband of the antenna, thereby enhancing the sideband selectivity. In addition, the current is reversed by loading shorting pin, and a radiation zero point is also introduced in the lower sideband. After measurement, the -10 dB impedance bandwidth of the filtering antenna is 23.6% (3.22-4.08 GHz), and the average antenna gain in the passband is 8.1 dBi. The filtering antenna does not involve an additional filter circuit, has a simple structure, and a small size, and ideally eliminates insertion loss. To verify, the real object was made and tested and found that the reflection coefficient, pattern, gain, etc. were in good agreement with the simulation results, it can be applied to the 5G communication frequency band.

Index Terms **–** 5G communication, filtering antenna, fractal structure, low profile, metasurface.

I. INTRODUCTION

In recent years, with the gradual development of portable mobile communication equipment, the miniaturization and integration of radio frequency front-end devices have become a research focus. The high-efficiency integrated design of the filter and the antenna can obtain a filtering antenna with good out-of-band suppression and high gain [1]. It integrates filtering and radiation functions and reduces the in-band loss caused by the mismatch between the filter and the antenna [2]. Therefore, the design of high-performance filtering antennas has very important practical significance for the further development of microwave circuit systems.

For example, in [3], the dual-mode rectangular SIW cavity is used as a high-Q common resonant cavity for the two bands, and then the filtering antenna is designed by using the orthogonally polarized SL cavity as the radiating element. However, this type of method requires multiple resonators to achieve filtering, which will occupy a large area and cause additional loss, thereby reducing antenna efficiency [4–6]. In [7], the transition structure from the micro-strip to the suture is used as the feed network of the antenna, and the planar dipole is used as the radiator. The filtering response is obtained by adding non-radiating elements to the feed network. Although these methods of adding parasitic bands on the feed network and adjusting the shape of the coupling hole to obtain the filtering effect avoid additional circuits, they still bring additional losses to a certain extent [8–11]. In addition, adding appropriate structures (such as etching grooves or adding short pins, parasitic bands, parasitic patches, etc.) to the antenna to insert the edge radiation zeros point can also achieve filtering characteristics [12–15]. Nowadays, metamaterials are widely used in some antenna designs due to their unique electromagnetic properties. Among them, compared with three-dimensional structural materials, metasurface has a smaller volume and lower loss and can be used in the design of high-performance antennas [16–18]. In [19], a series of non-uniform metal patches are used as the upper metasurface of the antenna, and the current misphase on the inner and outer sheets will produce a radiation zero point near the edge of the upper band. In [20], the researchers etched U-shaped gaps on the metasurface of the unit and loaded defective ground structures (DGS) on the ground to generate low-frequency radiation zeros. Therefore, a well-designed metasurface antenna can generate radiation zero points near the sidebands, thereby obtaining a low-profile, wide-band, and high-gain filtering antenna. Fractal geometry is introduced to design compact or multi-band electromagnetic structures due to the interesting features of space-filling and self-similarity [21]. Reasonable use of fractal structure can effectively improve the performance of microwave equipment, such as designing selective and compact antennas [22, 23].

To realize a better filtering response, in this paper, modifications are introduced both in the design of the metasurface and feeding circuit. Replacing the rectangular patch on the metasurface with a fractal patch can introduce a radiation zero point in the upper sideband of

Submitted On: June 16, 2022
Accepted On: January 2, 2023

https://doi.org/10.13052/2022.ACES.J.371106

the antenna. In addition, by loading a short PIN near the center of the ground to reverse the current on the surface of the patch, a radiation zero point can also be introduced in the lower sideband. To make the antenna exhibit good stop-band characteristics near high frequencies, it is also necessary to suppress its high-order modes, which can be achieved by adding stub micro-strip feeders and separation slots.

II. ANTENNA DESIGN AND ANALYSIS

Figure 1 is a schematic diagram of the three-dimensional structure of the designed filtering antenna. The filtering antenna is composed of a fractal metasurface and a feed network. The metasurface is set on the upper surface of the first layer of medium, the upper surface of the second layer of medium is a grounding plate with a rectangular gap, and the lower surface is a micro-strip feeder. Fig. 2 shows the configuration of the proposed filtering antenna. The optimized parameters of the antenna are shown in Table 1. Based on the slot-coupled micro-strip antenna, it adds stubs on the micro-strip feeder and separates the slots to suppress unwanted resonance modes in the antenna, thereby achieving a filtering effect. The simulation and analysis for the proposed filtering antenna are performed using the electromagnetic simulator ANSYS HFSS.

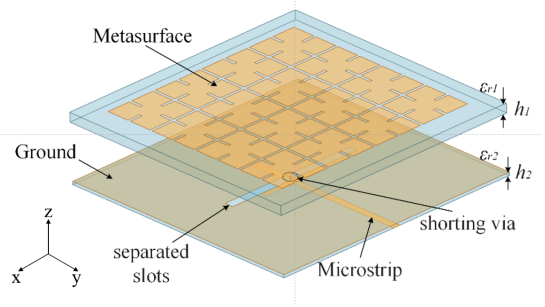

Fig. 1. The three-dimensional structure diagram of the proposed filtering antenna.

Table 1: Design parameters of the filtering antenna

Parameters	L_1	L_2	L_3	r
Values (mm)	18.85	10.7	8.525	0.2
Parameters	W_1	W_2	W_3	d
Values (mm)	2.5	1.95	1.8	0.2
Parameters	a	g	L	S
Values (mm)	6.5	0.8	70	0.8
Parameters	h_1	h_2	ε_{r1}	ε_{r2}
Values (mm)	2.6	0.813	2.2	3.38

To properly display the design concept of this filtering antenna, the following will analyze the mechanism of the antenna filtering response through five antenna structures.

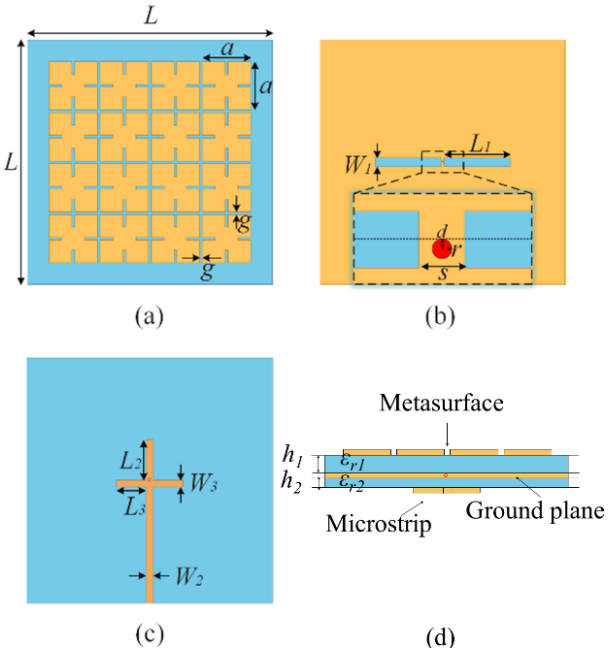

Fig. 2. Configurations of the proposed filtering antenna. (a) Metasurface. (b) Ground plate. (c) Feeder. (d) Side view.

The five structures are as follows: (I) The upper layer is a metasurface of the uniform rectangular patch and adopts linear micro-strip coupling feed. (II) Change the rectangular metasurface patches into fractal patches, and the feed structure remains unchanged. (III) The metasurface is made of fractal patches and two branches are added to the feeder. (IV) Separate the groove in the middle of structure III, and the metasurface structure remains unchanged. (V) A metal via is added in the middle of the groove separated in structure IV, and the other parts remain unchanged. Figure 3 lists several structures such as improved metasurfaces and feed networks. Among them, combining (a) and (b) with (c) respectively can get antennas (I) and (II), and combining (b) with (d), (e) and (f) in turn will get antennas (III), (IV) and (V). Simulate their reflection coefficient and gain curve in the electromagnetic simulation software in turn, and analyze the influence of each structural improvement on the antenna performance step by step.

To investigate the properties of the metasurface unit cell, the calculated reflection and transmission coefficients of the metasurface unit cell are shown in Fig. 4. The reflection coefficient magnitude is less than -10 dB in the whole simulation frequency range. On the other hand, the reflection coefficient phase varies from 0° to 180°, and it is close to stability at the working band

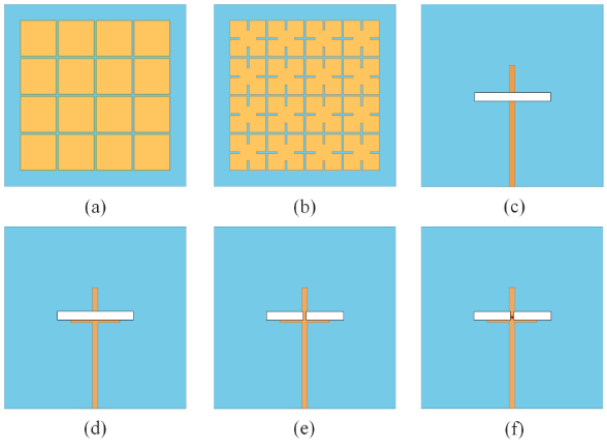

Fig. 3. Several antenna configurations. (a) The rectangular metasurface of Antenna I. (b) Fractal metasurfaces of antennas II, III, IV, and V. (c) Initial feeding circuit of antennas I and II. (d) Two additional arms are added to the linear micro-strip feeder of Antenna III. (e) Antenna IV is fed with two separate slots. (f) Antenna V has an additional shorting via.

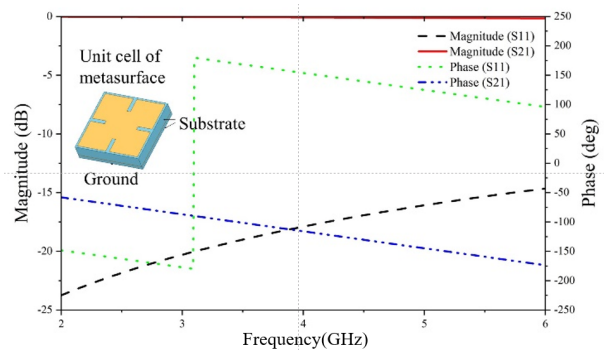

Fig. 4. Simulated reflection and transmission coefficient of the metasurface unit cell.

(3.22-4.08 GHz). It is indicated that the surface wave can propagate along the proposed metasurface.

Figures 5 (a) and (b) are respectively the $|S_{11}|$ and gain simulation curves of the antenna structure I-V. It can be found that with the improvement of the structure, Antenna V finally has a passband between 3.31-4.23 GHz. Compared with Antenna I, Antenna II is only modified from a rectangular metasurface to a fractal structure metasurface; however, the feed structure is the same. Its $|S_{11}|$ curve and gain curve have no change in the low-frequency part, but a weak radiation zero point appears at the frequency of 4.85 GHz. Antenna III has an improved feed structure based on Antenna II. It is found from Fig. 5 (a) that there is only one mode near 4.1 GHz. This shows that adding stubs to the linear feed structure can well suppress the high-frequency resonance mode of the antenna. Next, by adjusting the coupling gap to two separate grooves, the resonance condition of the gap can be destroyed, thereby suppressing the partial resonance near the low-frequency 2 GHz. In the end, the $|S_{11}|$ curve of the Antenna IV becomes smoother at low frequencies, but the sidebands of the curve are not very steep, resulting in poor roll-off characteristics. Try to add a radiation zero point similar to the upper sideband in the lower sideband to enhance its roll-off characteristics to achieve a good filtering effect. Therefore, add a shorting via in the middle of the two slots of Antenna IV to obtain Antenna V. The simulation results showed that it produces three resonance frequency points, and a radiation zero point appears at 3.18 GHz in Fig. 5 (b). Antenna V is the filtering antenna proposed in this paper. The average gain in the passband of the antenna is about 8dBi, there is no other resonance mode outside the band, which meets the design requirements of the filtering antenna.

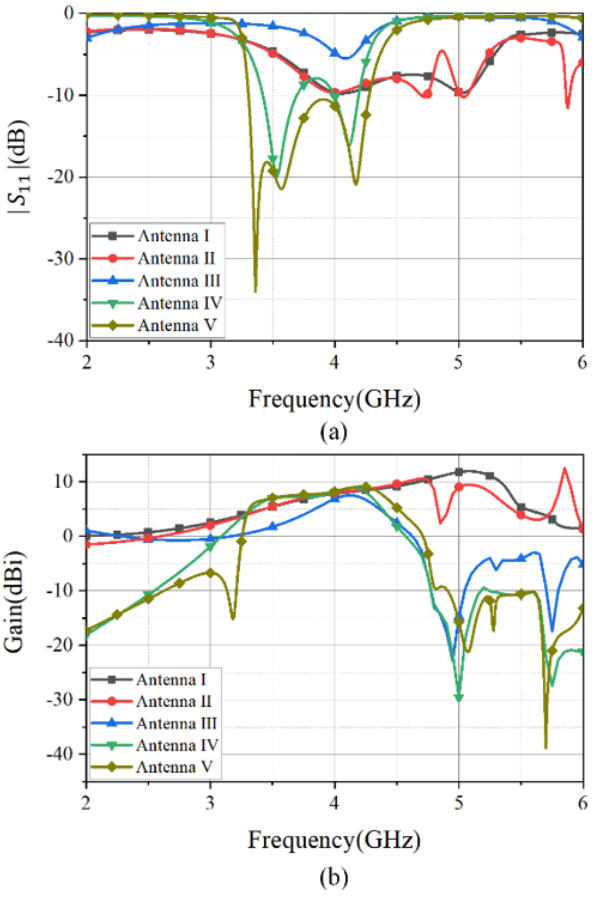

Fig. 5. The reflection coefficient $|S_{11}|$ and gain curves of the proposed five antennas are simulated. (a) $|S_{11}|$. (b) Gain.

To further analyze the generation principle of the antenna filtering response, the current distribution on the metasurface and ground plane of the five antenna

structures is given below. Figures 6 (a) and (b) show the current distribution of the metasurface of Antenna I and Antenna II at 4.85 GHz. Comparing them, the current direction on the rectangular metasurface is approximately the same. The direction of current on the outermost left and right rows of patches on the fractal metasurface is opposite to the direction of current on the two rows of patches in the middle. The radiation of the two can cancel each other, so a radiation zero point will be generated in the upper sideband. Figures 6 (c) and (d) are the current distribution of the ground plate of Antenna II and Antenna III at 4.7 GHz. The current of the Antenna II ground plate is not only concentrated on the micro-strip line but also distributed around the gap. The current of the Antenna III ground plate is only concentrated on the micro-strip line, and there is almost no energy around the gap. Therefore, the analysis shows that after adding the branch, the high-order mode of the antenna is suppressed, so that the rejection of the high-frequency range of the stop band is improved, and a good filtering effect is achieved. Figures 6 (e) and (f) are the current distributions of the metasurfaces of Antenna IV and Antenna V at 3.18 GHz. The current direction at the center of the metasurface of Antenna IV is uniformly downward, and when a shorting via is added at the center position, the current direction of Antenna V at this position is reversed, so a radiation zero point is also generated in the lower sideband.

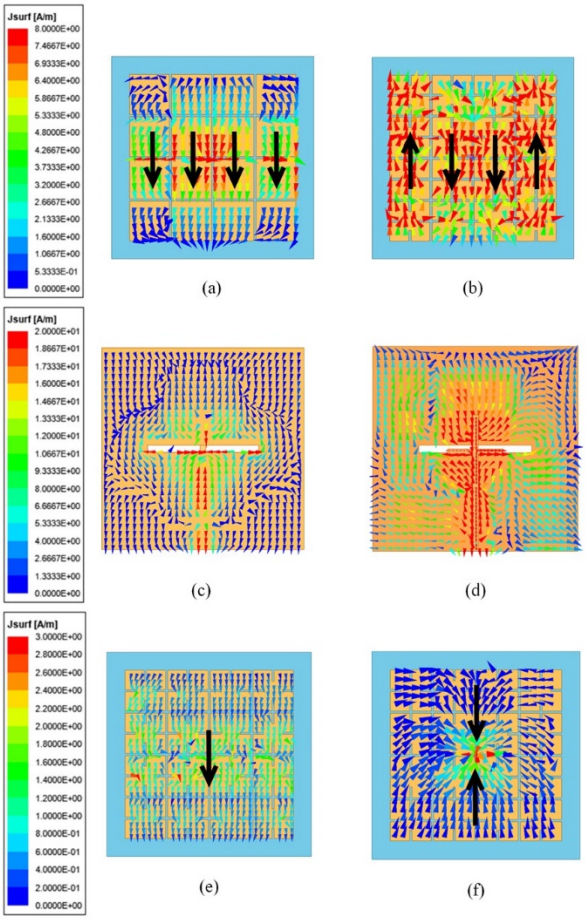

Fig. 6. Surface current distribution of the metasurface /ground plane of the filtering antenna. (a) Metasurface of Antenna I at 4.85 GHz. (b) Metasurface of Antenna II at 4.85 GHz. (c) Ground plane of Antenna II at 4.7 GHz. (d) Ground plane of Antenna III at 4.7 GHz. (e) Metasurface of Antenna IV at 3.18 GHz. (f) Metasurface of Antenna V at 3.18 GHz.

In the above content, the design principle of the filtering antenna is discussed, and then we will analyze the effect of the structural parameters on the performance of the filtering antenna. Figures 7 (a) and (b) show the reflection coefficient and gain of the filtering antenna under different slot lengths. As L_1 increases, the second resonant frequency point of the filtering antenna gradually moves to the low-frequency direction, and finally merges with the first frequency point. With the reduction of the slot length L_1, the out-of-band suppression of the antenna is improved to a certain extent, but the bandwidth is also relatively narrow. Therefore, the length of the gap on the ground plane should be moderate.

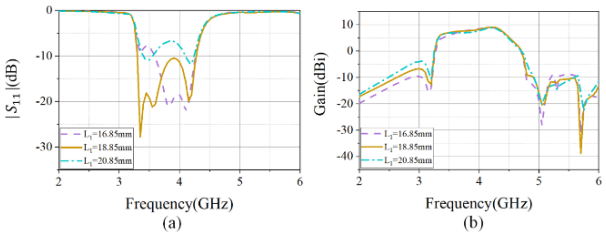

Fig. 7. (a) Simulated reflection coefficient of the filtering antenna for different slot lengths L_1. (b) Simulated gain of the filtering antenna for different slot lengths L_1.

Figures 8 (a) and (b) are simulation curves of the reflection coefficient and gain of the filtering antenna

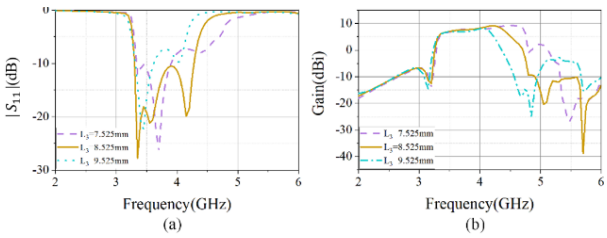

Fig. 8. (a) Simulated reflection coefficient of the filtering antenna for different arm lengths L_3. (b) Simulated gain of the filtering antenna for different slot lengths L_3.

under different arm lengths L_3. When L_3 is smaller, the third resonance mode at the high-frequency shifts to higher frequencies, and when it is larger, the working frequency band of the filtering antenna becomes narrower and partly above -10 dB. Therefore, an appropriate length of the short arm should be selected in the design process to ensure that the high-order mode of the antenna can be suppressed without affecting its bandwidth.

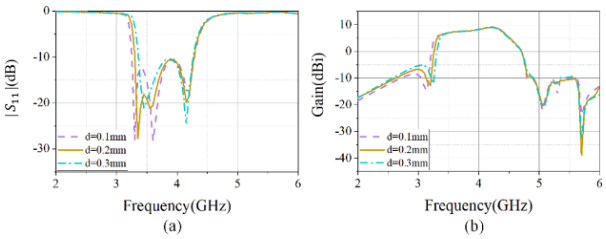

Fig. 9. (a) Simulated reflection coefficient of the filtering antenna for different short via positions. (b) Simulated gain of the filtering antenna for different short via positions.

To introduce a radiation zero point in the lower sideband of the antenna, a short via is set in the middle of the antenna separation slot. The location of the via also has a certain impact on the performance of the filtering antenna. Figures 9 (a) and (b) show the simulation curves of the reflection coefficient and gain of the filtering antenna when the distance d between the short via and the horizontal center line of the substrate changes. As the distance *d* increases, it can be seen that the bandwidth of the antenna and the resonance depth of the mode will slightly change, while the gain curve is almost unchanged. Therefore, to ensure processing accuracy and antenna bandwidth, the distance between the short via and the center line should be carefully selected.

III. MEASUREMENT VERIFICATION

To verify the performance of the designed filtering antenna, it was manufactured and tested. As shown in Fig. 10 , the upper metasurface is fabricated on an F4B dielectric substrate with a dielectric constant of 2.2 and a loss tangent of 0.003 (thickness 2.6 mm), and the lower layer uses Rogers 4003C with a dielectric constant of 3.38 and a loss tangent of 0.0027 as the dielectric substrate (thickness 0.813 mm).

The measurement of the proposed filtering antenna is shown in Fig. 11. The return loss was measured by using an Agilent E5071C vector network analyzer. Figure 12 shows the comparison curve between the measured value of the filtering antenna reflection coefficient and the simulated value. It can be seen that the measured curve is slightly shifted to the low frequency compared to the simulated curve. This may be because there is a gap between the two substrates during the physical processing and cannot fit together ideally. In addition, errors may

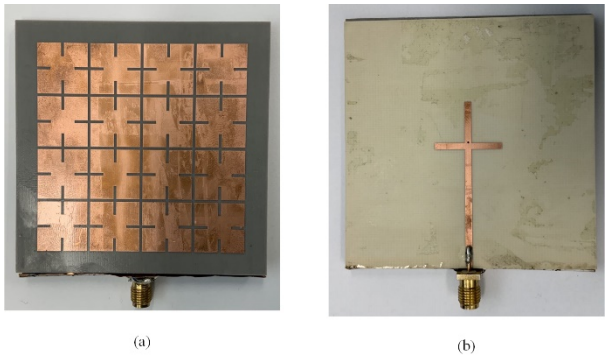

Fig. 10. Photographs of the fabricated filtering antenna. (a) Top view. (b) Bottom view.

Fig. 11. The measurement of the proposed filtering antenna.

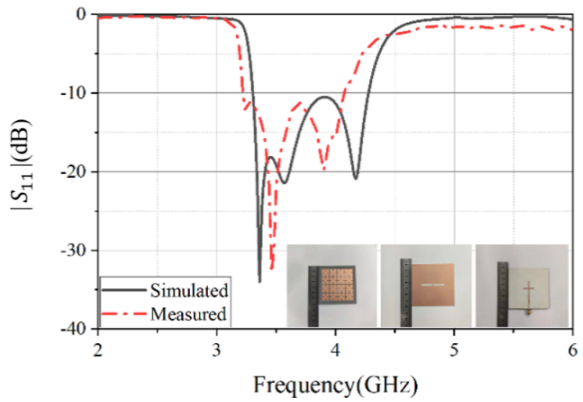

Fig. 12. Simulated and measured reflection coefficients of the filtering antenna.

be introduced during the measurement process, which may also cause deviations between the simulation results and the actual measurement results. The sidebands of the simulated curve and the measured curve are relatively steep, and both show good filtering characteristics. Among them, the measured -10dB impedance bandwidth

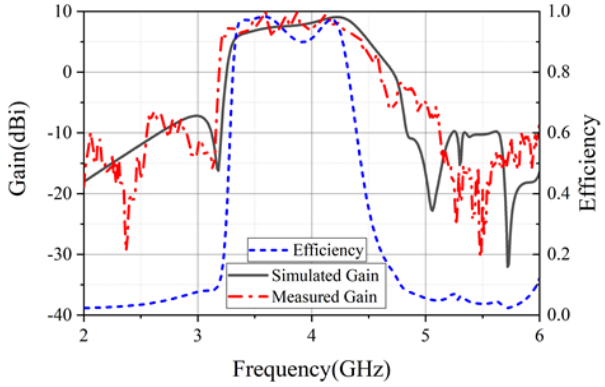

Fig. 13. Simulated and measured the gain of the filtering antenna and efficiency simulation values.

is 23.6% (3.22-4.08 GHz), and the simulated -10 dB impedance bandwidth is 24.4% (3.31-4.23 GHz), and there is not much difference between them. In Fig. 12, the comparison curve between the measured gain value and the simulated value of the proposed filtering antenna and the antenna efficiency is given. It can be seen that although the measured gain curve has a slight jitter compared to the simulated gain curve, the overall consistency is better. In addition, it can be seen that the antenna has a radiation zero point at 3.18 GHz and 5.05 GHz. These two radiation zero points enhance the sideband roll-off of the antenna and bring good edge selectivity. In the range of 3.31-4.23 GHz, the average gain of the filtering antenna reached 8.1 dBi, while the gain dropped rapidly outside the sideband. In the lower stopband range of 2.0-3.18 GHz, the antenna achieves an out-of-band rejection of nearly 17 dB. In the higher stopband range of 5.05-6 GHz, an out-of-band rejection of more than 20 dB is achieved. In addition, the average in-band efficiency of the antenna exceeds 90%, reaching 98.5% at the highest point.

Figure 14 depicts the normalized radiation pattern of the filtering antenna at the three resonance points of 3.35 GHz, 3.60 GHz, and 4.20 GHz. The simulation results are in good agreement with the measured results.

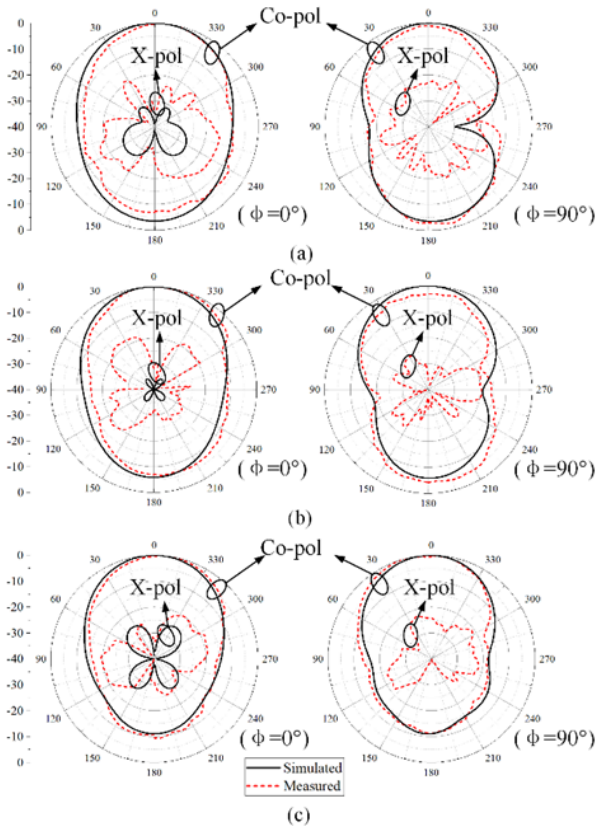

Fig. 14. Simulated and measured normalized radiation patterns of the filtering antenna. (a) The normalized pattern of the filtering antenna at 3.35 GHz. (b) The normalized pattern of the filtering antenna at 3.60 GHz. (c) The normalized pattern of the filtering antenna at 4.20 GHz.

In addition, it can be seen from Fig. 14 that the main polarization of the measured H plane (xz plane) and E plane (yz plane) is approximately 25 dB greater than the cross-polarization. It should be noted that the cross-polarization obtained by simulation is less than -40 dB. The performance comparison between the filtering antenna proposed in this article and other reported filtering antennas is given in Table 2. In contrast, our

Table 2: Comparison between the proposed filtering antenna and some previous works

References	**Center Frequency (GHz)**	**Profile (λ_0)**	**FBW(%)**	**Average Gain (dBi)**	**Suppression Level (dB)**	**Size (λg*λg)**
[8]	4.22	0.078	61.4	8.7	23	0.84*0.84
[12]	4.5	0.098	22.6	7.4	23	0.66*0.66
[15]	2.4	0.032	20.1	9.5	14.5	1.2*1.2
[19]	5	0.06	28.4	8.2	20	1.3*1.3
[20]	7	0.04	17.6	8	17	0.77*0.77
This work	3.35	0.038	23.6	8.1	17	0.78*0.78

proposed filtering antenna based on the fractal metasurface unit achieves a broadband filter response under the condition of low profile ($0.038\lambda_0$). In addition, the antenna has a relatively high gain in the passband and a satisfactory suppression level in the stopband.

IV. CONCLUSION

In this paper, a filtering antenna based on a metasurface is designed by using a slot-coupled feeding mode. The working principle of the antenna is analyzed through the surface current, and the function of each structure of the antenna is explained. The antenna has a good filtering effect. To verify the performance of the filtering antenna, the actual antenna was fabricated and measured. The -10 dB impedance bandwidth measured by the filtering antenna is 23.6% (3.22-4.08 GHz), its structure is compact, and the profile is low. The average gain in the antenna passband is 8.1 dBi and the efficiency exceeds 90%, which can meet the needs of 5G communication. Regardless, future research should be devoted to the development of filtering properties by well-designed fractal metasurface and compacting its structure further.

ACKNOWLEDGMENT

This work was supported by the State Key Program of National Natural Science of China (Grant No. 61631007), the Nation Key R&D Program of China (Grant No. 2019YFA0405403), and the Lanzhou University Innovation and Entrepreneurship Project (Grant No. cxcy202002). In addition, I would also like to thank Prof. Zhonglei Mei and A/Prof. Guoping Gao for their help in measuring instruments during the actual measurement phase.

REFERENCES

[1] Q. Liu, L. Zhu, J. Wang, and W. Wu, "A wideband patch and SIW cavity hybrid antenna with filtering response," *IEEE Antennas and Wireless Propagation Letters*, vol. 19, no. 5, pp. 836-840, 2020.

[2] Y. Li, Z. Zhao, Z. Tang, and Y. Yin, "Differentially fed, dual-band dual-polarized filtering antenna with high selectivity for 5G Sub6 GHz base station applications," *IEEE Trans. Antennas Propagat.*, vol. 68, no. 4, pp. 3231-3236, 2020.

[3] K. Dhwaj, H. Tian, and T. Itoh, "Low-profile dual-band filtering antenna using common planar cavity," *IEEE Antennas and Wireless Propagation Letters*, vol. 17, no. 6, pp. 1081-1084, 2018.

[4] C. X. Mao, S. Gao, Y. Wang, and Z. Cheng, "Filtering antenna with two-octave harmonic suppression," *IEEE Antennas and Wireless Propagation Letters*, vol. 16, pp. 1361-1364, 2017.

[5] L. S. Wu, Y. X. Guo, J. F. Mao, and W. Y. Yin, "Design of a substrate integrated waveguide balun filter based on three-port coupled resonator circuit model," *IEEE Microwave and Wireless Components Letters*, vol. 21, no. 5, pp. 252-254, 2011.

[6] X. J. Lin, Z. M. Xie, P. S. Zhang, and Y. Zhang, "A broadband filtering duplex patch antenna with high isolation," *IEEE Antennas and Wireless Propagation Letters*, vol. 16, pp. 1937-1940, 2017.

[7] Y. Zhang, X. Y. Zhang, and Y. M. Pan, "Low-profile planar filtering dipole antenna with omnidirectional radiation pattern," *IEEE Trans. Antennas Propagat.*, vol. 66, no. 3, pp. 1124-1132, 2018.

[8] P. F. Hu, Y. M. Pan, X. Y. Zhang, and S. Y. Zheng, "Broadband filtering dielectric resonator antenna with wide stopband," *IEEE Trans. Antennas Propagat.*, vol. 65, no. 4, pp. 2079-2084, 2017.

[9] B. J. Xiang, S. Y. Zheng, Y. M. Pan, and Y. X. Li, "Wideband circularly polarized dielectric resonator antenna with bandpass filtering and wide harmonics suppression response," *IEEE Trans. Antennas Propagat.*, vol. 65, no. 4, pp. 2096-2101, 2017.

[10] X. Y. Zhang, Y. Zhang, Y. M. Pan, and W. Duan, "Low-profile dual band filtering patch antenna and its application to LTE MIMO system," *IEEE Trans. Antennas Propagat.*, vol. 65, no. 1, pp. 103-113, 2017.

[11] W. Duan, X. Y. Zhang, Y. M. Pan, J. X. Xu, and Q. Xue, "Dual-polarized filtering antenna with high selectivity and low cross polarization," *IEEE Trans. Antennas Propagat.*, vol. 64, no. 10, pp. 4188-4196, 2016.

[12] W. Yang, Y. Zhang, W. Che, M. Xun, Q. Xue, G. Shen, and W. Feng, "A simple, compact filtering patch antenna based on mode analysis with wide out-of-band suppression," *IEEE Trans. Antennas Propagat.*, vol. 67, no. 10, pp. 6244-6253, 2019.

[13] J. Y. Jin, S. Liao, and Q. Xue, "Design of filtering-radiating patch antennas with tunable radiation nulls for high selectivity," *IEEE Trans. Antennas Propagat.*, vol. 66, no. 4, pp. 2125-2130, 2018.

[14] X. Y. Zhang, W. Duan, and Y. M. Pan, "High-gain filtering patch antenna without extra circuit," *IEEE Trans. Antennas Propagat.*, vol. 63, no. 12, pp. 5883-5888, 2015.

[15] D. Yang, H. Zhai, C. Guo, and H. Li, "A compact single-layer wideband microstrip antenna with filtering performance," *IEEE Antennas and Wireless Propagation Letters*, vol. 19, no. 5, pp. 801-805, 2020.

[16] G. Feng, L. Chen, X. Xue, and X. Shi, "Broadband surface-wave antenna with a novel nonuniform tapered metasurface," *IEEE Antennas and Wireless Propagation Letters*, vol. 16, pp. 2902-2905, 2017.

[17] W. Zhang, Y. Liu, and Y. Jia, "Circularly polarized antenna array with low RCS using metasurface-inspired antenna units," *IEEE Antennas and Wireless Propagation Letters*, vol. 18, no. 7, pp. 1453-1457, 2019.

[18] G. N. Zhou, B. H. Sun, Q. Y. Liang, Y. H. Yang, and J. H. Lan, "Beam Deflection short backfire antenna using phase-modulated metasurface," *IEEE Trans. Antennas Propagat*., vol. 68, no. 1, pp. 546-551, 2020.

[19] Y. M. Pan, P. F. Hu, X. Y. Zhang, and S. Y. Zheng, "A low-profile high-gain and wideband filtering antenna with metasurface," *IEEE Trans. Antennas Propagat*., vol. 64, no. 5, pp. 2010-2016, 2016.

[20] W. Yang, S. Chen, Q. Xue, W. Che, G. Shen, and W. Feng, "Novel filtering method based on metasurface antenna and its application for wideband high-gain filtering antenna with low profile," *IEEE Trans. Antennas Propagat*., vol. 67, no. 3, pp. 1535-1544, 2019.

[21] C. Borja, G. Font, S. Blanch, and J. Romeu, "High directivity fractal boundary microstrip patch antenna," *Electronics Letters*, vol. 36, no. 9, pp. 778-779, 2000.

[22] S. Zheng, Y. Yin, J. Fan, X. Yang, B. Li, and W. Liu, "Analysis of miniature frequency selective surfaces based on fractal antenna–filter–antenna arrays," *IEEE Antennas and Wireless Propagation Letters*, vol. 11, pp. 240-243, 2012.

[23] T. Cai, G. M. Wang, X. F. Zhang, and J. P. Shi, "Low-profile compact circularly-polarized antenna based on fractal metasurface and fractal resonator," *IEEE Antennas and Wireless Propagation Letters*, vol. 14, pp. 1072-1076, 2015.

Jingci Zhu received a B.E. degree in communication engineering from Tianjin University, Tianjin, China, in 2020. He is currently pursuing a master's degree in Information and Communication Engineering at the School of Information Science and Engineering, Lanzhou University. His current research interests are in the area of wireless communications, with a focus on antenna technology, digital pre-distortion linearization (DPD), and spread spectrum system design.

Guanmao Zhang received a B.S. degree from Lanzhou University, Lanzhou, China, in 1995, an M.S. degree in Radio Physics from Lanzhou University in 1998, and the Ph.D. degree in radio physics from Lanzhou University in 2007.

He is currently the director of the Institute of Optoelectronics and Electromagnetic Information, School of Information Science and Engineering, Lanzhou University. His current research interests include surface plasmonics and its communication sensor applications, micro-nano optical device design and application, non-intrusive intelligent photoelectric sensor technology and application, and modern wireless communication technology. At present, he has published more than 40 related academic papers, of which more than 20 are included in SCI/EI.

Zhihang Li received a B.E. degree in communication engineering from Shandong University, Shandong, China, in 2019. He is currently pursuing a master's degree in Electronic and Communication Engineering at the School of Information Science and Engineering, Lanzhou University. His current research interests include frequency selective surfaces, periodic structures, and metamaterial absorbers.

Zonge Che received a B.E. degree in electronic information engineering from Lanzhou Jiaotong University, Lanzhou, China, in 2019. She is currently pursuing a master's degree in Information and Communication Engineering at the School of Information Science and Engineering, Lanzhou University. Her current research interests include terahertz filters, surface plasmonics, metasurface, and metamaterial absorber.

Juan Yue in Communication Engineering from Bohai University, Jinzhou, China, in 2018. She is currently pursuing a master's degree in information and communication engineering at the School of Information Science and Engineering, Lanzhou University. Her current research interests include microstrip filters and metamaterial absorbers.

Yinhai Feng received a B.E. degree in electronic information engineering from Zhengzhou University, Zhengzhou, China, in 2019. He is currently pursuing a master's degree in information and communication engineering at, the School of Information Science and Engineering, Lanzhou University. His current research interests include circularly polarized antennae and multifrequency antennae.

Qian Zhang received a B.E. degree in Electronic Information Engineering from Yantai University, Yantai, China, in 2020. She is currently pursuing a master's degree in Information and Communication Engineering at the School of Information Science and Engineering, Lanzhou University. Her current research interests include surface plasmonics metasurface, periodic structures, and metamaterial absorbers.

Rui Qiu received a B.E. degree in Communication Engineering from Southwest Minzu University, Sichuan, China, in 2021. He is currently pursuing a master degree in electronic and communication engineering, School of Information Science and Engineering, Lanzhou University. His current research interests include Terahertz metalens, vortex beam generator and surface plasmonics metasurface.